



DFT study on $X^-(H_2O)_n$ ($X = OH, NO_2, NO_3, CO_3$) anionic water cluster



M. Lalitha, L. Senthilkumar*

Department of Physics, Bharathiar University, Coimbatore 641046, Tamil Nadu, India

ARTICLE INFO

Article history:

Accepted 21 October 2014

Available online 27 October 2014

Keywords:

Anion

Water cluster

Solvation energy

Energy decomposition analysis

AIM

NBO

ABSTRACT

A theoretical study to understand the interaction between anion and the water molecules through the hydration $(X^-(H_2O)_n)$ ($X = OH, NO_2, NO_3, CO_3$), where $n = 1-10$, using the density functional theory method with B3LYP functional and 6-311++G(d,p) basis set has been carried out systematically. In these hydrated clusters we notice three different cases of bond arrangements, namely, symmetrical double hydrogen bond, single hydrogen bond and inter-water hydrogen bond. All the complexes are dominated by the $O-H \cdots O$ hydrogen bond, in which the anion act as a proton acceptor, while the water molecule act as a proton donor. A linear correlation is obtained between the solvent stabilization energy and the size (n) of the hydrated cluster for all the anions. The weighted average interaction energy values, shows that the water molecules strongly bind with the OH^- anion. Besides, the solvation of the OH^- anion requires less number of water molecules when compared with the other anions. Energy decomposition analysis (EDA) shows the strong dominance of the electrostatic energy component within the interaction energy. The total NPA charges on the anions indicate an increase in the solvation due to hydration. From AIM analysis, excellent linear inverse correlation is observed for both the electron density and Laplacian of the electron density with respect to the hydrogen bond length. Natural bonding orbital analysis (NBO) predicts large charge transfer between the OH^- anion and the water molecules.

© 2014 Elsevier Inc. All rights reserved.

1. Introduction

Understanding the chemistry of the hydrated anions are highly important because of its relevance in both the basic and the applied sciences (hydrogen bonding, solvation and nucleation) [1–3]. Anions like OH^- , O_2^- , HO_2^- , NO_2^- , CO_3^- , NO_3^- , HCO_4^- , $NO_3^-(HNO_3)_2$, etc., are related with the important problems like the origin of ice crystals in the Antarctic stratosphere, the evolution of the positive and the negative cluster ions in both the stratosphere and the troposphere [4,5]. Existence of several dominant series of hydrated ions in the troposphere has been confirmed by few research groups [6–8] using the mass spectrometric analysis. Besides, both positive and negative charged water clusters are known to exist at all levels of the atmosphere including the troposphere, stratosphere and ionosphere.

Study on the microhydration of small anionic species is of great interest, because, the hydrated complexes formed between the anion and the water molecules can provide insight on the role of anions in the chemical and the atmospheric processes.

Likewise, the microhydration can also address issues regarding structure-energetics relations, the existence of anion on the surface or in the interior of water clusters, which subsequently can improve our understanding of the molecular level interactions between the solvent water molecules and the negatively charged ions in the aqueous solution. However, the anion solvation is more complicated since most of the anion-water interactions are generally weaker and energetically comparable with the water–water interactions. As a consequence, a delicate balance between the anion-water and the water-water interactions is crucial in determining the bulk vs. surface solvation, i.e., structures with the anion on the “surface” of water clusters [9]. Similarly, the difficulty in predicting the structures of the hydrated anions due to number of geometries is also inevitable [10]. Furthermore, extensive experimental as well as theoretical [11–15] study limits the anionic water clusters in the order of three to five water molecules, since the sensitivity of the negative clusters typically extends to four hydrates at room temperature [16]. However, the recent literatures related to hydration of anion have shown only few theoretical works on the hydration of the hydroperoxide and the hydroxyl ions. Like, Anick [17] explored the structure of gas phase $(HOO^-(H_2O)_n)$ clusters at B3LYP/6-311++G** level of theory, and found that (HOO^-) enhances the hydrogen bonding network, whereas $HOOH$ disrupts

* Corresponding author. Tel.: +91 9443702753.

E-mail address: lsenthilkumar@buc.edu.in (L. Senthilkumar).

the hydrogen bonding network. Likewise, molecular dynamics study on the aqueous HOO^- ion by Ma et al. [18] highlights the importance of four HOO^- hydration species in water at ambient temperature. Further, study of transient hydrogen bond in the $\text{OH}^-(\text{H}_2\text{O})_4$ and $\text{OH}^-(\text{H}_2\text{O})_3$ complexes by Aziz et al. [19] report that the hydration structure of the hydroxide ion cannot be inferred from that of the hydrated excess proton. Likewise, Ma and Tuckerman [20] performed ab initio molecular dynamics calculations on OH^- reorientation and transport as a function of temperature. Similarly Mundy et al. [21] predicted the stabilization of the hydroxide anion at the air–water surface relative to bulk water. Furthermore, Hassanali et al. [22] explored the mechanisms of the recombination of hydronium and hydroxide ions in liquid water using ab initio molecular dynamics simulations. In general, all the above studies reiterate the importance of the hydration of anions.

Based on the above details, we have selected four singly charged anions namely the diatomic linear type anion, OH^- , the triatomic bend type anion NO_2^- and the tetra-atomic, cyclic type anions NO_3^- and CO_3^- due to their unique role in the chemical and the atmospheric sciences. For instance, OH^- anions in the solutions describe the pH value of the solution and determine the physico-chemical properties of the acid and the base solution. In the chemical reactions, these ions behave as a reacting species, as well as ionizing agents [26]. Further, Nitrate anion (NO_3^-) also known as terminal or Hofmeister anion, is one of the most abundant species in acidic wastes as well as in the atmosphere [27,28]. Lastly, NO_2^- is a source of hydroxyl radical through its photodecomposition and also along with CO_3^- as negative atmospheric ions have long lifetimes in air (>1 s) [29,30].

Density functionals developed for covalent systems are largely successful in treating hydrogen bonding as well as noncovalent interactions that act over similarly short length scales (<2 Å) [23]. In contrast, the dispersion attraction, which arises from correlated motions of electrons, is prominent over longer distances [~ 2 – 5 Å (medium-range) and >5 Å (long-range)] [24,25]. From the studies of Anick et al. [17], Ma et al. [18] and Mundy et al. [21] it is implied that the DFT functionals B3LYP and BLYP are well suited to study the hydrogen bonded network.

In the present work, we employed density functional theory methodology to study the effect of hydration on OH^- , NO_2^- , NO_3^- and CO_3^- anions. For this the number of water molecules hydrating these anions is varied from 1 to 10 with notation $\text{X}^-(\text{H}_2\text{O})_{n=1-10}$ ($\text{X} = \text{OH}, \text{NO}_2, \text{NO}_3, \text{CO}_3$). The constructed cluster geometry for this study is solely for solvating anion rather than shape or symmetry.

2. Computational methods

The structure of the $\text{X}^-(\text{H}_2\text{O})_{n=1-10}$ ($\text{X} = \text{OH}, \text{NO}_2, \text{NO}_3, \text{CO}_3$) clusters has been studied in a systematic way using the density functional theory methodology. Geometry optimization has been performed with hybrid density functional, namely, B3LYP and the basis set 6-311++G(d,p) with two diffuse function and polarization function, in accordance with the published results in the literature, which indicate that this above functional and basis set are good enough to study hydrogen bonded systems [31,32] and to find the minimum energy structure. B3LYP has generally been the method of choice to study the hydrogen-bonded systems, as it includes correlation with reasonable compromise between size and reliability. Earlier studies [33,34] have shown that the B3LYP/6-311++G(d,p) level of theory predict the hydrogen bond length and angle for the ionic structures with accuracy (mean absolute error of approximately 0.02 Å), than the other DFT methods. Thus B3LYP/6-311++G(d,p) level of theory is well suited to study the geometries and energies of the anionic-water clusters.

The harmonic vibrational frequency analysis [35] confirms the global minima state of the optimized structures.

The interaction energies and solvent stabilization energies of the clusters are also calculated. With the increase in the number of solvent water molecules in the hydrated clusters, the number of minimum energy configurations that are close in energy is anticipated to increase. Therefore, the weighted average properties of clusters become more meaningful. Weighted average molecular properties have been calculated based on the statistical population of the possible minimum energy configurations of a particular size of hydrated cluster at 150 K, since the spectroscopy experiments are mostly carried out around this temperature [36]. Besides, on the basis of free energy change at 150 K, the population of the minimum energy configurations of the each size cluster is calculated. Natural population analysis (NPA) is noted in order to get a better view about the charge distribution in anions due to hydration. Natural Bond Orbital (NBO) analysis has been carried out using NBO 3.1 program at the same level of theory to study the charge transfer [37]. All the computations were carried out using Gaussian 03 package [38]. The partition of interaction energy and the nature of hydrogen bonds formed in the anionic water clusters are studied using energy decomposition analysis (EDA) implemented in GAMESS software [39,40]. Further, the interaction energy (from EDA) has been corrected for BSSE (Basis Set Superposition Error) error, using the Boys and Bernardi counterpoise method [41]. The hydrogen bonds are characterized by the topological parameters obtained by the theory of atoms in molecules (AIM) of Bader using the program MORPHY [42].

3. Results and discussion

The optimized structure of the anions OH^- , NO_2^- , NO_3^- and CO_3^- along with its NPA atomic charges (in a.u.) in the gas phase are displayed in Fig. 1a–d, respectively. The calculated bond distances of the anions are as follows; O–H in OH^- is 0.967 Å, N–O in NO_2^- , NO_3^- are 1.258 Å and 1.260 Å respectively, while the C–O bond length in CO_3^- is 1.273 Å. The sum of the total NPA atomic charges of each anion comes to -1 , as it is singly charged anion. Further, the chosen anions are hydrated by discrete sized water molecules ($n = 1$ – 10) in various possible geometries, according to the chemical intuition. Presumably, the hydrated structure considered here either encloses the anion within or restrains the anion along the plane. Moreover, the structures with more than five water molecules are not reported in the literature. The number of possible configurations of an anion with each water molecule is limited to three or four. Based on the above, we obtained 128 computed geometries for all the anion–water complexes, 24 structures belong to $\text{OH}^-(\text{H}_2\text{O})_n$, 33 structures for $\text{NO}_2^-(\text{H}_2\text{O})_n$, 23 complexes for $\text{NO}_3^-(\text{H}_2\text{O})_n$ and 25 complexes belongs to $\text{CO}_3^-(\text{H}_2\text{O})_n$. For the purpose of analysis and convenience, we have examined only the most stable structures from each discrete sized anion–water complex. The selected most stable geometries of $\text{OH}^-(\text{H}_2\text{O})_n$, $\text{NO}_2^-(\text{H}_2\text{O})_n$, $\text{NO}_3^-(\text{H}_2\text{O})_n$ and $\text{CO}_3^-(\text{H}_2\text{O})_n$ are displayed in Figs. 2–5

, respectively. The systems are labelled as (X^-)_{wn}-hm, where, X^- denotes the anion ($\text{X} = \text{OH}, \text{NO}_2, \text{NO}_3, \text{CO}_3$), wn gives the number of water molecules bonded with anion and hm represents the possible geometries for the particular wn.

3.1. Structure

All the anion–water complexes are formed solely through O–H...O hydrogen bond, except for NO_2^- anion, in which O–H...N hydrogen bond is observed in addition. In all the hydrogen bonds between the anion and the water molecules, the anion acts as proton acceptors while the water molecule is the proton donor.

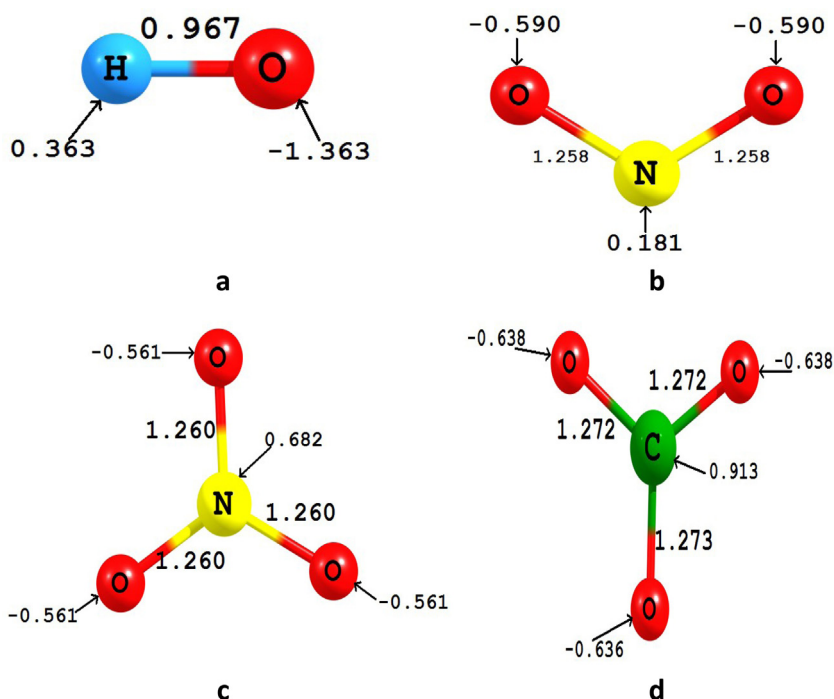


Fig. 1. Optimized geometries of (a) OH^- , (b) NO_2^- , (c) NO_3^- and (d) CO_3^{2-} anions calculated at the B3LYP/6-311++G(d,p) level of theory illustrating the bond lengths (in Å) and the NPA atomic charges (in e).

Moreover, the hydrogen bond between the anion and the water molecules, which involves both anion-water and water-water interactions are classified into three types as (i) symmetric double hydrogen bonding (DHB), in which two H-atoms of the solvent H_2O molecule are attached to two different atoms of the anion. (ii) Single Hydrogen Bonding (SHB), in which one H-atom of the water molecule is bonded to any one of the atoms of the anion and (iii) inter-water hydrogen bonding (WHB). However, in the first hydration shell the anions directly co-ordinate with the water molecule through both SHB and DHB. Thereafter, the second hydration shell of the cluster solely involves WHB. On an average, the anions form 1 to 6 hydrogen bonds directly with the water molecules in its first solvation shell. Each of the four anions considered forms at most 17 hydrogen bonds in total with the water molecules in their respective ten water complexes. From the above sections we observe two classes of the hydrogen bonds formed in the clusters: (a) interaction between the anion and the water molecules and (b) interaction between the water molecules in the first hydration shell and the other water molecules. However, in the foregoing results and discussion, we focus only on the hydrogen bond interaction between the anion and the water molecules in the first hydration shell.

3.2. OH^-

Optimized structure of the isolated OH^- anion along with its NPA charges displayed in Fig. 1a has an O–H bond length as 0.967 Å. The most stable configurations of each discrete sized hydrated complex are displayed in Fig. 2. All the $\text{OH}^-(\text{H}_2\text{O})_n$ systems are formed by the SHB and the WHB, but there is no DHB, because spectroscopic studies [43,44] of aqueous alkali metal hydroxides provide information on the structure of the OH^- anion in solution, which indicates that the OH^- group is not strongly bonded through its hydrogen, but makes intermolecular water contacts through its oxygen [45]. However, OH^- anion in its first solvation shell forms 4 hydrogen bonds, with four water molecules [46,47].

Table S1 (given in supporting information, SI) shows the optimized bond length and bond angle values for hydrogen bond

between OH^- and H_2O in the most stable configurations of $\text{OH}^-(\text{H}_2\text{O})_n$ complexes. Hydrogen bond lengths in $\text{OH}^-(\text{H}_2\text{O})_n$ complexes ranges from 1.362 Å to 1.821 Å and its corresponding bond angles are 176.60° and 175.33° . The strongest hydrogen bond length of 1.362 Å occurs in monohydrated complex (OH^-) w1-h1, and its bond angle is highly linear, while the weakest hydrogen bond length of 1.821 Å occurs in complex (OH^-) w8-h2. In addition, the structure of monohydrated complex (OH^-) w1-h1 is different from other structures, in which one of the hydrogen's in water is shared as a proton between the two OH group, eventually forming three fragment structure of the form $[\text{HO} \cdots \text{H} \cdots \text{OH}]^-$ [48].

3.3. NO_2^-

The optimized structural parameters along with NPA charges of isolated NO_2^- ion shown in Fig. 1b has N–O bond distance as 1.258 Å and the O–N–O bond angle is 116.75° . The NPA charges are distributed around the oxygen atoms of the anion than the nitrogen atom, since the oxygen part of the anion is more reactive to the water molecules. NO_2^- in its first solvation shell forms maximum of five hydrogen bonds with five water molecules. The most stable structures of discrete sized $\text{NO}_2^-(\text{H}_2\text{O})_n$ clusters are displayed in Fig. 3. All the complexes of $\text{NO}_2^-(\text{H}_2\text{O})_n$ are formed by SHB and WHB, while the DHB occurs only in the structures having one and two water molecules. In higher clusters, to accommodate more water molecules, the anion prefers only SHB. Each oxygen atom of the NO_2^- anion forms two SHB, while nitrogen can form single SHB, thus the NO_2^- anion is able to form five SHB in total. The optimized bond length and bond angle values of hydrogen bond formed between NO_2^- and H_2O in the most stable configurations of discrete sized $\text{NO}_2^-(\text{H}_2\text{O})_n$ complexes are tabulated in Table S2 of SI. Hydrogen bond length of $\text{NO}_2^-(\text{H}_2\text{O})_n$ system varies from 1.715 Å to 2.146 Å. The strong hydrogen bond length occurs in the system (NO_2^-) w10-h2 with the bond length of 1.715 Å and the bond angle of 174.73° , which is highly linear. A weak hydrogen bond length of 2.146 Å occurs in the system (NO_2^-) w2-h3 with the bond angle of 136.67° . Among the most stable configurations,

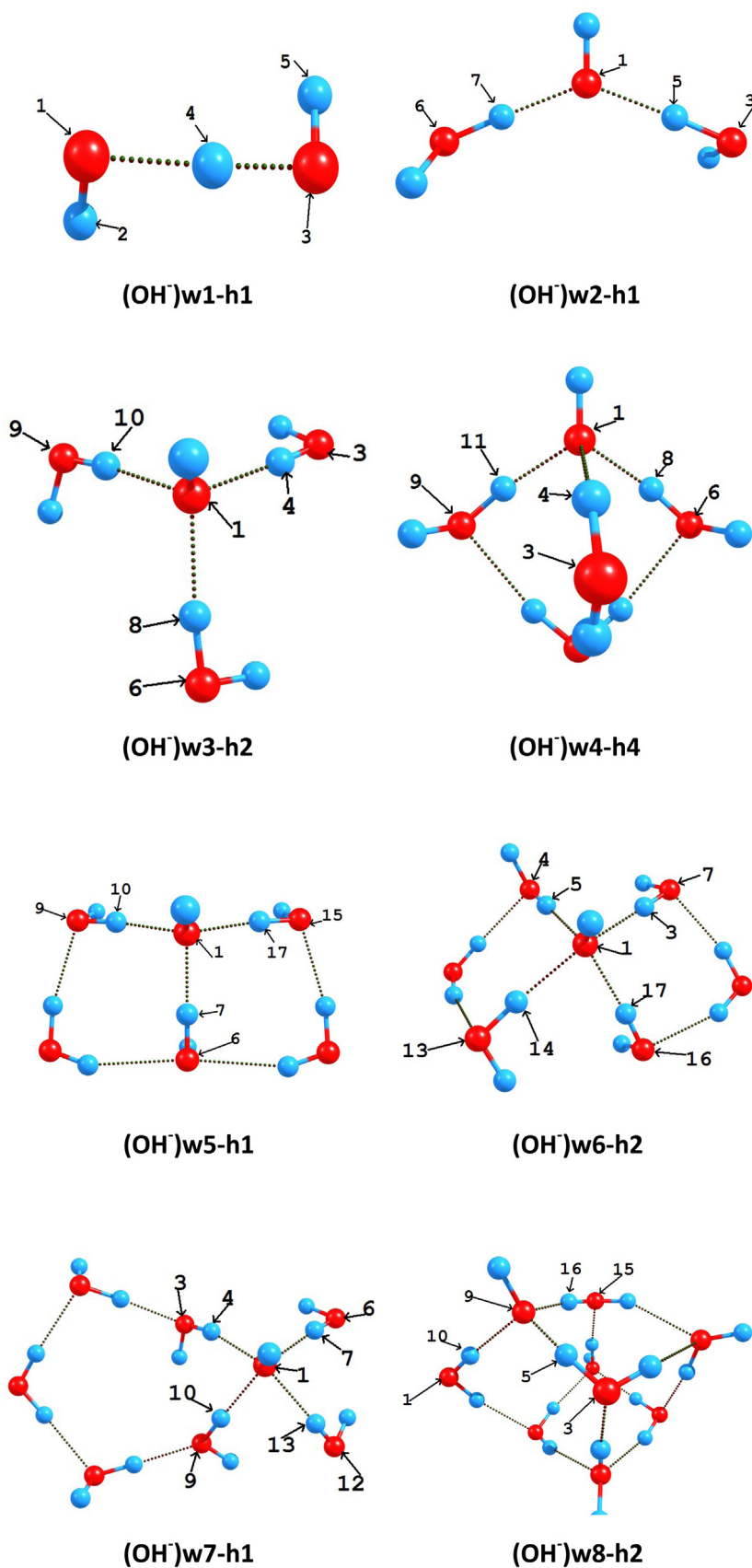


Fig. 2. The optimized geometry of the most stable configurations of $\text{OH}^- \cdot (\text{H}_2\text{O})_n$, where $n = 1-10$. The atoms numbered with arrow are involved in the hydrogen bond between anion and water molecule. The blue and red balls indicate hydrogen and oxygen atoms respectively.

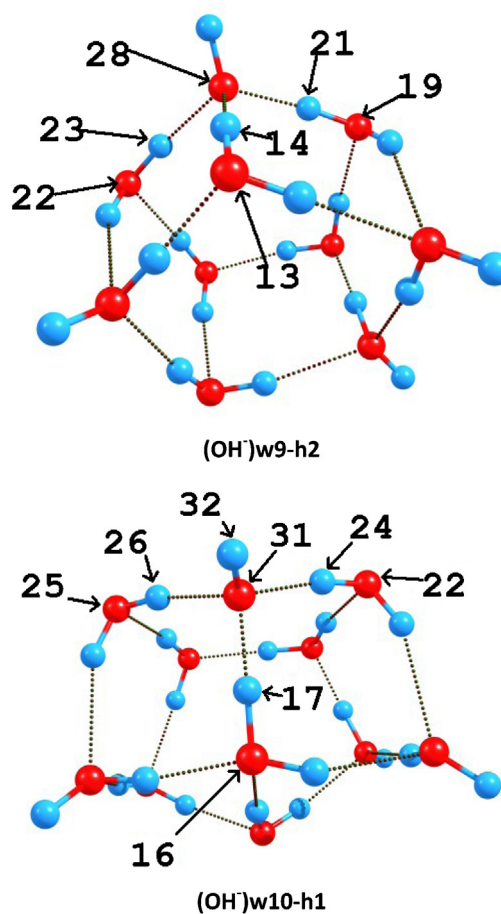


Fig. 2. (Continued).

the O–H...N hydrogen bond occurs in the (NO_2^-) w8-h3 with the bond length of 1.946 Å and in (NO_2^-) w9-h2 with 1.808 Å.

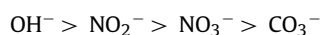
3.4. NO_3^-

Optimized geometry of isolated nitrate anion with its NPA atomic charge distributions shown in Fig. 1c has N–O bond distance as 1.260 Å and O–N–O bond angle of 120°. The figure illustrates that all the three oxygen atoms are equally negative. The effect of hydration on the nitrate anion is measured by the successive addition of discrete solvent H_2O molecules. When a solvent H_2O molecule approaches the solute NO_3^- anion, an ionic interaction between the negatively charged oxygen atom of NO_3^- and the H atom of solvent H_2O takes place. NO_3^- in its first solvation shell forms maximum of 6 hydrogen bonds in the first solvation shell for three as well as six water molecules in the structures (NO_3^-) w3-h1 and (NO_3^-) w6-h1 respectively. Most stable structures of each discrete sized $\text{NO}_3^- \cdot (\text{H}_2\text{O})_n$ clusters are displayed in Fig. 4. As there are three oxygen atoms in NO_3^- , the possibility of SHB in the anion-water complex also increases. Presumably, NO_3^- anion can form a maximum of six SHB with water molecules (2 SHB per oxygen atom), after which the complex grows solely by WHB. The DHB is observed in complexes having water molecules from 1 to 3. The optimized bond length and bond angles of hydrogen bonding between NO_3^- and H_2O for the most stable complexes of $\text{NO}_3^- \cdot (\text{H}_2\text{O})_n$ are tabulated in Table S3 of SI. The hydrogen bond length of $\text{NO}_3^- \cdot (\text{H}_2\text{O})_n$ clusters varies from 1.689 Å to 2.364 Å, and its corresponding bond angles varies from 173.47° to 126.21° which occurs in systems (NO_3^-) w4-h2 and (NO_3^-) w3-h1, respectively.

3.5. CO_3^-

Fig. 1d shows the optimized geometry along with NPA charges of isolated CO_3^- ion, where the C–O bond distance of CO_3^- anion is 1.272 Å, and the O–C–O bond length is 120°. The NPA atomic charges show that negative charges are evenly distributed on the oxygen atoms of the anion and subsequently, there is a possibility of forming DHB between the anion and the water molecule. CO_3^- in its first solvation shell forms maximum of 6 hydrogen bonds in its first solvation shell with six water molecules. The most stable structures of $\text{CO}_3^- \cdot (\text{H}_2\text{O})_n$ are displayed in Fig. 5. Complex (CO_3^-) w1-h2 forms a DHB with water molecule, and further addition of water molecules results in SHB with the anion. Similar to NO_3^- , CO_3^- is also able to form six SHB in total. The corresponding bond length and bond angle values of the hydrogen bonds in the most stable complexes of $\text{CO}_3^- \cdot (\text{H}_2\text{O})_n$ clusters are tabulated in Table S4 of SI. The strong hydrogen bond length of 1.777 Å occurs in (CO_3^-) w4-h2 with the bond angle of 175.52°. The weak hydrogen bond length occurs in the system (CO_3^-) w1-h2 with the bond length and bond angle of 2.428 Å and 127.19°, respectively.

Thus, from the structural analysis, it is visible that the some of the hydrogen bond length values in the NO_2^- , NO_3^- and CO_3^- water clusters exceed 2 Å, on the contrary for OH^- anion, all the hydrogen bond length values are less than 2 Å. This concludes that the OH^- anion interacts strongly with the water molecules. Further, the strength of hydrogen bond in the anionic cluster is independent of the number of water molecules. Overall, the anion order based on the hydrogen bond length from strong to weak is as follows:



From the above, the higher order of the OH^- anion is due to the presence of the donor and acceptor pair O and H, which are capable of forming strong hydrogen bonds. In addition, the hydrogen-bonded network in OH^- anionic cluster is only through SHB and WHB. It is also worth to mention here that bond order strength follows the electronegativity

order of the anions, which is based on the absolute values (in eV),

$$\text{OH}^-(2.935) > \text{NO}_2^-(2.477) > \text{NO}_3^-(1.6112) > \text{CO}_3^-(1.2332)$$

Among the three types of hydrogen bonding considered, SHB and DHB occurs only with the anion, whereas WHB is the inter-

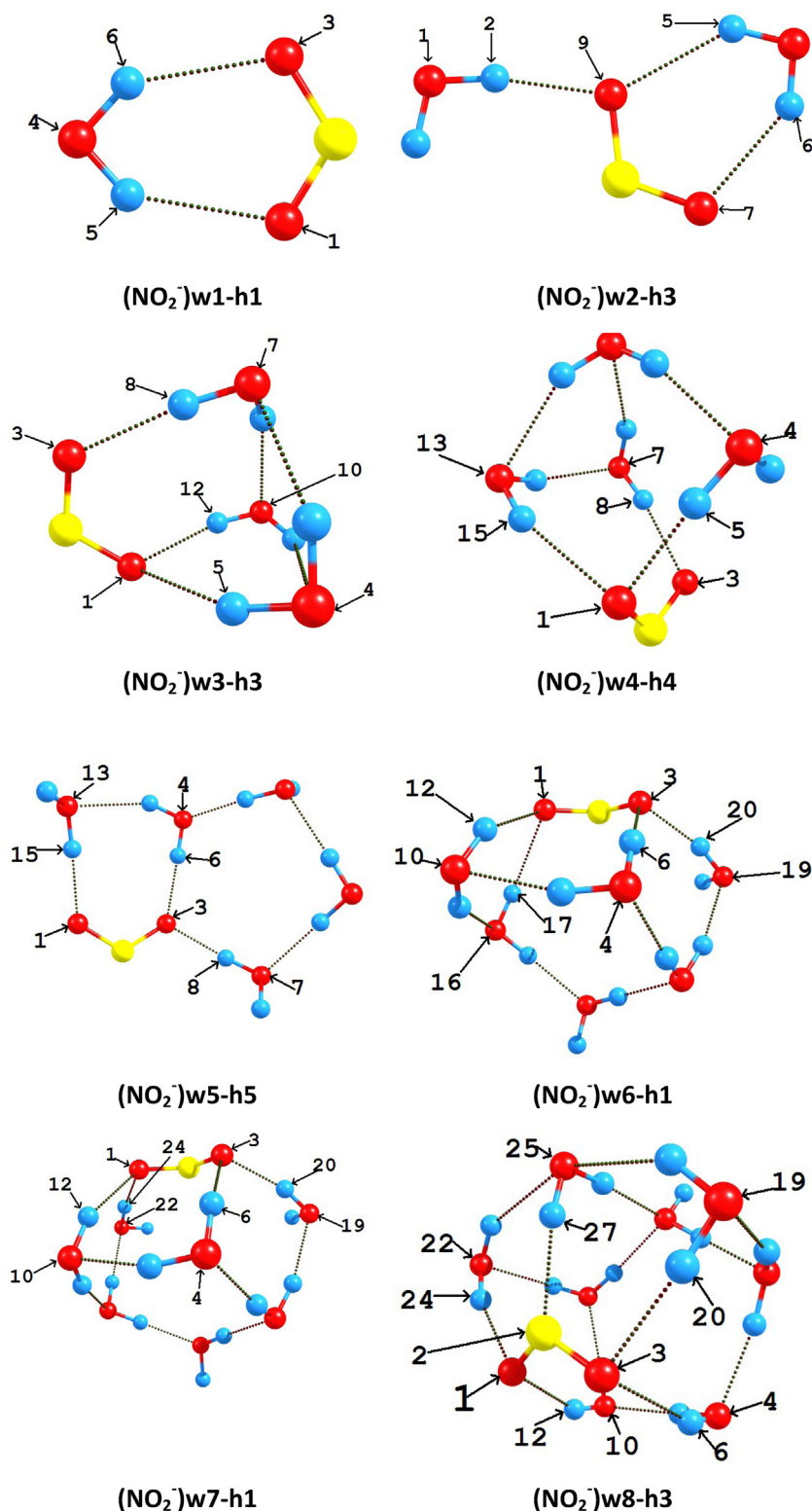


Fig. 3. The optimized geometry of the most stable configurations of $\text{NO}_2^-(\text{H}_2\text{O})_n$, where $n=1-10$. The atoms numbered with arrow are involved in the hydrogen bond between anion and water molecule. The blue, red and yellow balls indicate hydrogen, oxygen and nitrogen atoms respectively.

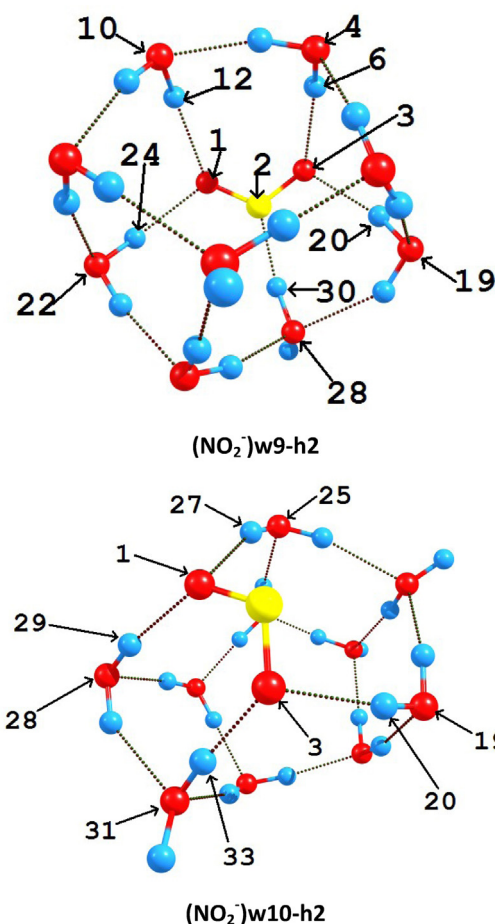


Fig. 3. (Continued).

water hydrogen bonding (does not occur with the anion). The first solvation shell of the anion consists of both SHB and DHB, whereas the WHB occurs only in the further solvation shells. In general, the bond length of WHB formed in the OH^- anion-water complexes is comparably greater than the anion-water bond length, indicating that the hydrogen bonded network is weaker than the anion-water bonds.

3.6. Solvent stabilization and interaction energy

Solvent stabilization energy and interaction energy of all the discrete sized hydrated anions are calculated, in order to get a clear view about the influence of hydration on anion stabilization and interaction. The solvent stabilization energy (E^{solv}), i.e., the stabilization induced by solvent water molecules of $\text{X}^-(\text{H}_2\text{O})_n$ clusters can be expressed by the relation,

$$E^{\text{solv}} = E_{\text{X}^-(\text{H}_2\text{O})_n} - (nE_{\text{H}_2\text{O}} + E_{\text{X}^-})$$

where X^- refer to the anions, OH^- , NO_2^- , NO_3^- and CO_3^- and n stands for the number of water molecules. The energy parameters $E_{\text{X}^-(\text{H}_2\text{O})_n}$, $E_{\text{H}_2\text{O}}$ and E_{X^-} refer to the total energy of the cluster with the respective anions ($\text{X}^-(\text{H}_2\text{O})_n$), the energy of a single water molecule and the energy of the bare anion (X^-) respectively. Thus, E^{solv} essentially measures the total interaction energy of the solute with n solvent H_2O units in the hydrated cluster of size n [28].

Interaction energy refers to the net interaction between solute anion and the solvent water molecules eliminating inter-water interactions. Interaction energy (E^{int}) defines the interaction

between the anion, X^- ($\text{X} = \text{OH}^-$, NO_2^- , NO_3^- , CO_3^-) and the water cluster, is calculated by the following relation,

$$E^{\text{int}} = E_{\text{X}^-(\text{H}_2\text{O})_n} - (E_{(\text{H}_2\text{O})_n} + E_{\text{X}^-})$$

The energy parameters $E_{\text{X}^-(\text{H}_2\text{O})_n}$, $E_{(\text{H}_2\text{O})_n}$ and E_{X^-} refer to the energy of the total complex, the energy of the water molecules within the complex and the energy of the anion within the complex respectively. The interaction energy is BSSE corrected using the Boys and Bernardi counterpoise method [41].

The solvation energy and the interaction energy of the discrete sized hydrated anionic clusters are calculated at the B3LYP/6-311++G(d,p) level of theory and are tabulated in Table S5, S6, S7 and S8 for $\text{OH}^-(\text{H}_2\text{O})_n$, $\text{NO}_2^-(\text{H}_2\text{O})_n$, $\text{NO}_3^-(\text{H}_2\text{O})_n$ and $\text{CO}_3^-(\text{H}_2\text{O})_n$ respectively in the Supporting Information (SI). Since for the each size of the cluster, several minimum energy configurations are obtained (24 structures for $\text{OH}^-(\text{H}_2\text{O})_n$, 33 structures for $\text{NO}_2^-(\text{H}_2\text{O})_n$, 23 complexes for $\text{NO}_3^-(\text{H}_2\text{O})_n$ and 25 complexes for $\text{CO}_3^-(\text{H}_2\text{O})_n$), therefore calculated weighted average solvation energy (E_w^{solv}) and interaction energy (E_w^{int}) values provide a better view on the solvation properties. The weight factor for the minimum energy structure of a particular cluster size (n) is calculated using the statistical population of the conformer at 150 K, following Boltzmann distribution. The variation of the weighted average solvation energy (E_w^{solv}) and interaction energy (E_w^{int}) values with the number of water molecules are shown in Table 1 and plotted in Fig. 6a–d for the $\text{OH}^-(\text{H}_2\text{O})_n$, $\text{NO}_2^-(\text{H}_2\text{O})_n$, $\text{NO}_3^-(\text{H}_2\text{O})_n$ and $\text{CO}_3^-(\text{H}_2\text{O})_n$ clusters, respectively. Numerical energy values are reported in the above-mentioned tables and the figures, but for the foregoing discussion, we refer only to the absolute energy

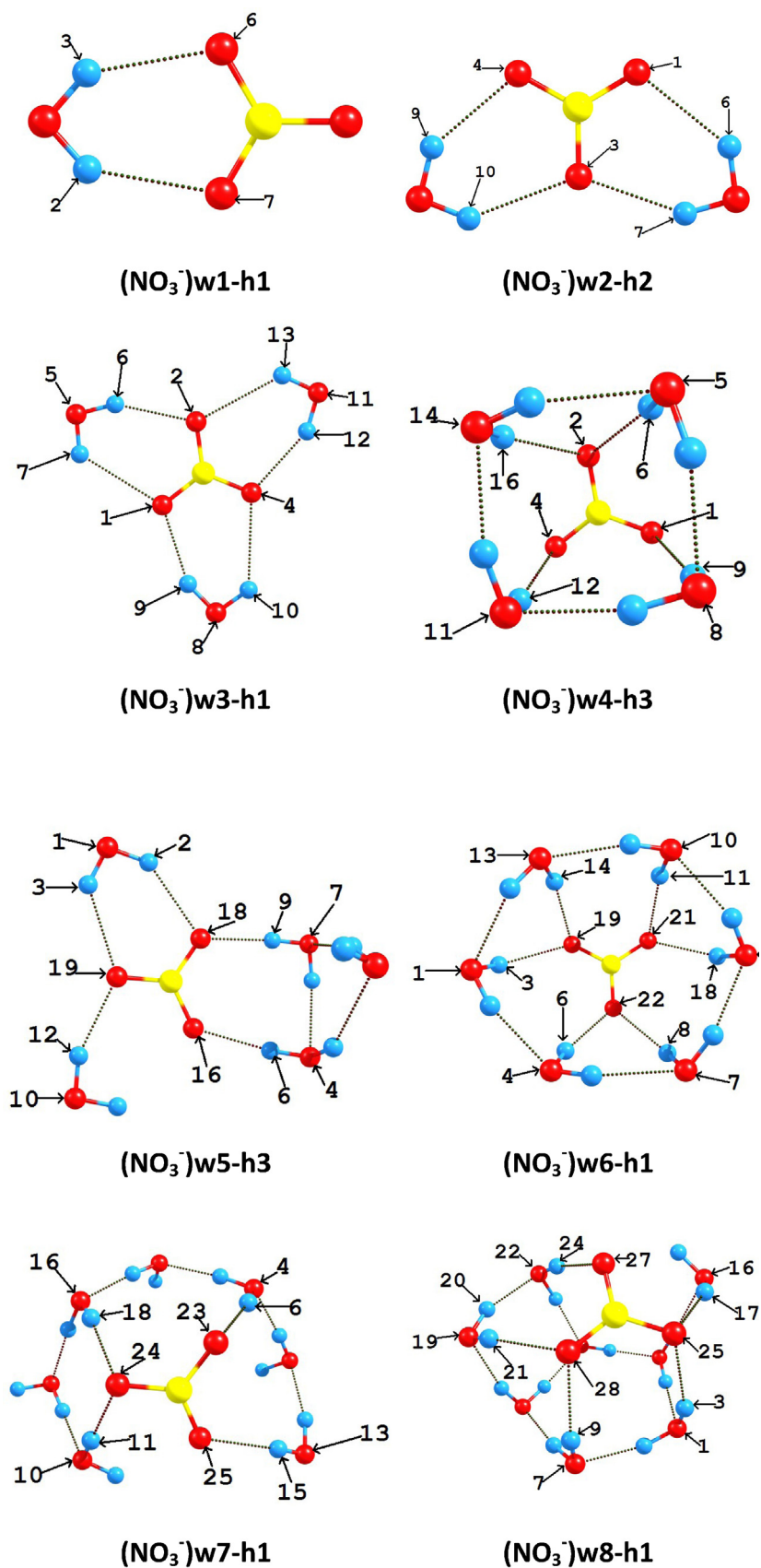


Fig. 4. The optimized geometry of the most stable configurations of NO₃⁻·(H₂O)_n, where $n=1-10$. The atoms numbered with arrow are involved in the hydrogen bond between anion and water molecule. The blue, red and yellow balls indicate hydrogen, oxygen and nitrogen atoms respectively.

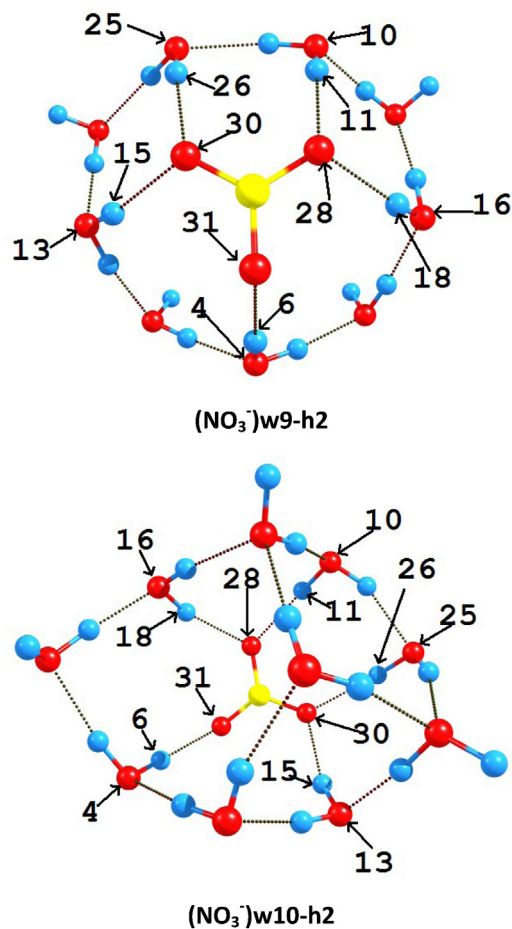


Fig. 4. (Continued).

values. From the solvation energy plot for all the anionic systems, the observed characteristics are (i) E_w^{solv} linearly increases with the number of solvent water molecules in the hydrated clusters. (ii) E_w^{solv} values does not saturate, which hints that additional water molecules can be coordinated with the existing water network.

All the above observations are common, but for the better understanding of the solvation of each anion by the water molecules, it is important to calculate the stabilization provided by the water molecule to each anion. For this the linear fit analysis could be an intuitive tool. For the $\text{OH}^-\cdot(\text{H}_2\text{O})_n$ anionic systems, variation of E_w^{solv} values is best fitted as, $E_w^{solv} = 26.415 + 13.916n$, where E_w^{solv} is the solvation energy in kcal/mol and n is the number of water

molecules. The slope value suggests that the solvent stabilization energy per water molecule is 13.916 kcal/mol. This indicates that if the addition of each water molecule provides an increase in the number of H-bonds by 2, then on an average each additional H-bond provides stabilization energy of 6.958 kcal/mol at a larger n limit. Similarly the linear fit for the $\text{NO}_2^-\cdot(\text{H}_2\text{O})_n$ anionic system is $E_w^{solv} = 6.143 + 12.407n$, and here water molecule provides the solvent stabilization energy of 12.407 kcal/mol. In other words, each additional H-bond provides stabilization energy of 6.203 kcal/mol at a larger n limit, which is slightly lower than the OH^- anion. In the case of the NO_3^- hydrated clusters the linear fit $E_w^{solv} = 0.484 + 12.452n$, suggests that an additional water

Table 1
Calculated weighted average solvation and interaction energy of $\text{OH}^-\cdot(\text{H}_2\text{O})_n$, $\text{NO}_2^-\cdot(\text{H}_2\text{O})_n$, $\text{NO}_3^-\cdot(\text{H}_2\text{O})_n$ and $\text{CO}_3^-\cdot(\text{H}_2\text{O})_n$, ($n = 1-10$) complexes at the B3LYP/6-311++G (d,p) level of theory.

| Cluster size | Weighted average property (kcal/mol) | | | | | | | |
|--------------|--------------------------------------|-------------|------------------------------|-------------|------------------------------|-------------|------------------------------|-------------|
| | OH ⁻ | | NO ₂ ⁻ | | NO ₃ ⁻ | | CO ₃ ⁻ | |
| | E_w^{solv} | E_w^{int} | E_w^{solv} | E_w^{int} | E_w^{solv} | E_w^{int} | E_w^{solv} | E_w^{int} |
| 1 | -29.39 | -37.49 | -17.28 | -17.58 | -14.05 | -14.14 | -13.07 | -13.18 |
| 2 | -52.79 | -56.07 | -31.79 | -32.32 | -29.18 | -29.96 | -26.48 | -27.31 |
| 3 | -72.29 | -74.92 | -45.10 | -46.50 | -41.80 | -43.10 | -36.90 | -38.20 |
| 4 | -86.00 | -86.95 | -56.84 | -54.76 | -41.19 | -50.88 | -48.55 | -46.38 |
| 5 | -102.40 | -99.81 | -67.86 | -60.52 | -61.33 | -58.20 | -59.37 | -52.73 |
| 6 | -116.14 | -109.66 | -78.08 | -67.96 | -72.80 | -62.80 | -69.36 | -60.23 |
| 7 | -125.20 | -115.57 | -96.15 | -54.56 | -87.40 | -51.30 | -81.10 | -56.30 |
| 8 | -137.39 | -120.64 | -98.80 | -41.00 | -101.08 | -39.64 | -90.80 | -66.70 |
| 9 | -149.17 | -124.75 | -119.38 | -52.04 | -114.46 | -54.24 | -101.00 | -69.70 |
| 10 | -158.81 | -131.48 | -132.55 | -58.22 | -126.39 | -58.42 | -124.09 | -55.86 |

molecule induces a stabilization energy of 12.452 kcal/mol. Correspondingly, each additional hydrogen bond with the water molecule provides a stabilization energy of 6.226 kcal/mol, which on comparing with the OH^- anion is marginally less, but greater

than the NO_2^- anion. For the $\text{CO}_3^{2-} \cdot (\text{H}_2\text{O})_n$ anionic systems the linear fit $E_{\text{W}}^{\text{sol}} = 1.806 + 11.503n$, indicates that the solvent stabilization energy per solvent water molecule for the CO_3^{2-} anion is 11.503 kcal/mol, which shows that each hydrogen bond provides

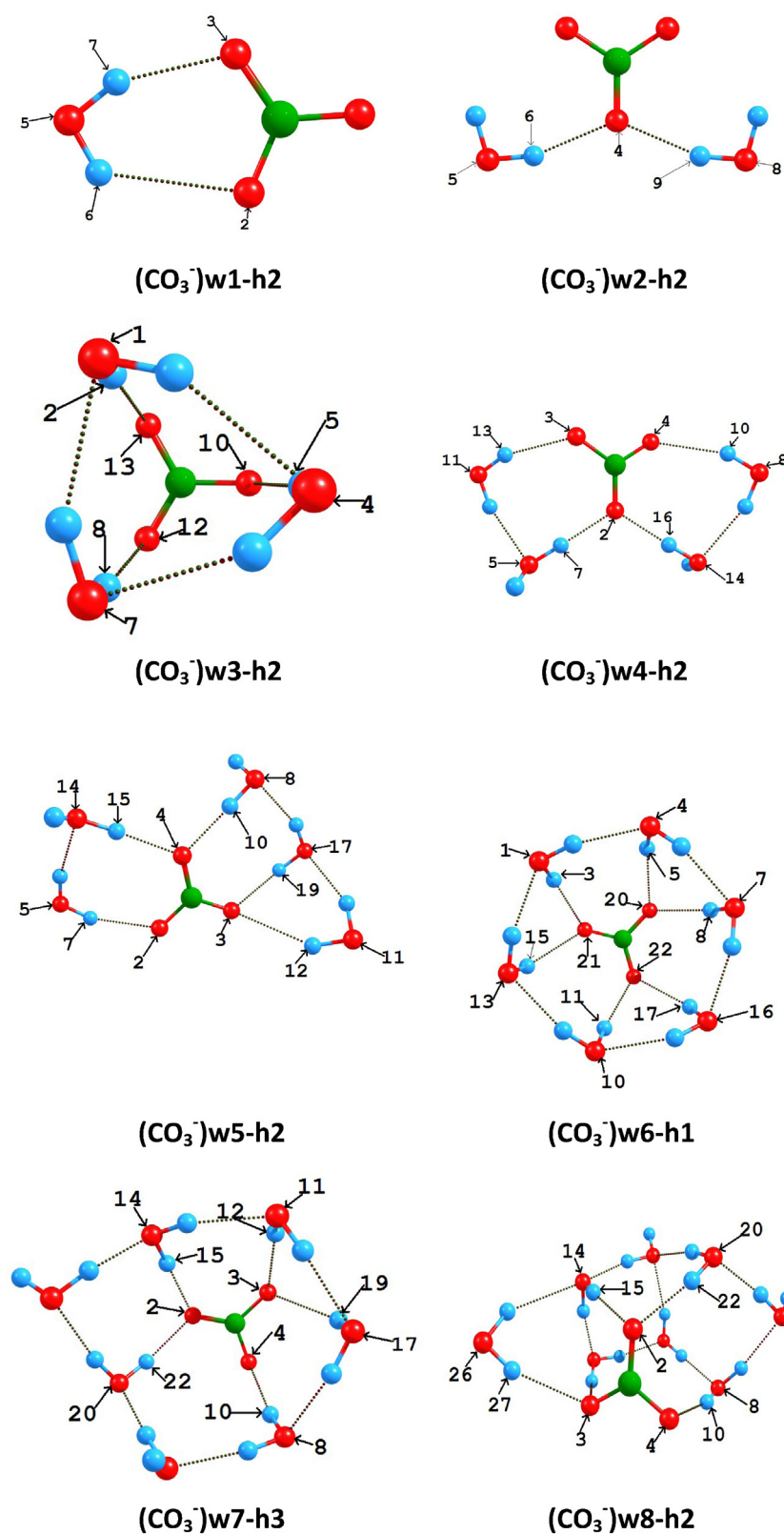


Fig. 5. The optimized geometry of the most stable configurations of $\text{CO}_3^{2-} \cdot (\text{H}_2\text{O})_n$, where $n=1-10$. The atoms numbered with arrow are involved in the hydrogen bond between anion and water molecule. The blue, red and green balls indicate hydrogen, oxygen and carbon atoms respectively.

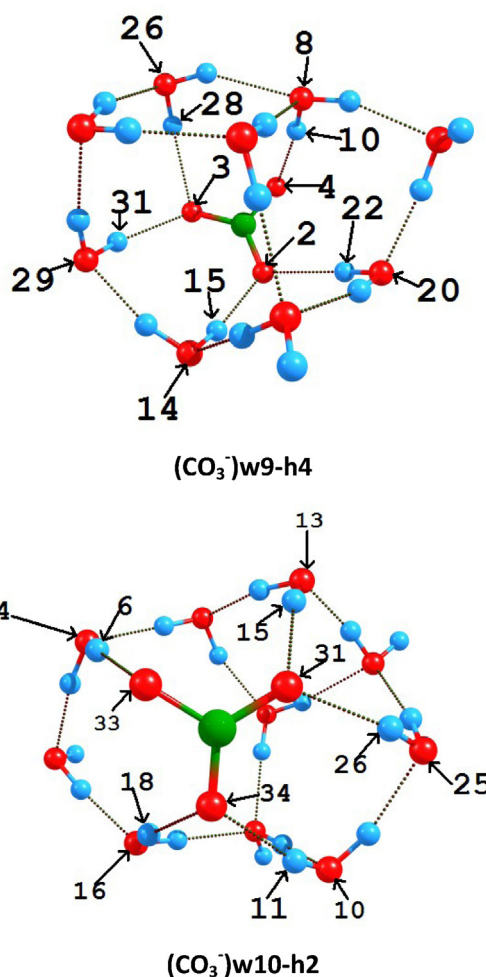


Fig. 5. (Continued).

a stabilization energy of 5.751 kcal/mol at a large n limit, which is also the least stabilization energy among the four anions. Based on the magnitude of the hydrogen bond stabilization energy of all the anions, the order obtained is as follows:



The above results and the order indicates that each hydrogen bond provides more energy for the OH^- anion to get stabilized and therefore lesser number of hydrogen bonds is needed for the OH^- anion to get solvated, than the other anions. This also indicates that the interaction between the OH^- anion with water is stronger and more attractive than the other anions.

Further, from the solvent stabilization energy results it is important to study the strength of the attractive interaction between the anions and the water molecules. Hence, the weighted average interaction energy (E_w^{int}) are calculated for all the anion-water cluster sizes on the basis of the statistical population at 150 K and the corresponding results are supplied in Table 1. From the figures of the weighted average interaction energy (E_w^{int}) given in Fig. 6a–d, it is observed that the E_w^{int} values for all the anions increases with the increase in the number of solvent water molecules, except for a few stable structures. Particularly, for the OH^- anion there is a linear increase in the interaction energy, which also overlaps with the solvation energy up to $n=6$ water molecules. For the NO_2^- , NO_3^- and CO_3^{2-} anions, the interaction energy is very close to the solvation energy up to the size of $n=4$, because the water molecules are directly bonded with the anion. However, beyond $n=4$ the addition

of further water molecules increases the cluster size by coordinating with the water molecules rather than the anions. Subsequently, the calculated interaction energy after $n=4$ is lower in value than the solvent stabilization energy. This reiterates that the inter-water hydrogen bonding is significant after $n=6$ and $n=4$ for OH^- and NO_2^- , NO_3^- , CO_3^{2-} , anion-water complexes respectively. To conclude, from the weighted average interaction energy values, the anion OH^- binds strongly with the water molecules in comparison with the other anions.

3.7. Natural population analysis (NPA) charges

The analysis of atomic charges on the anion within the hydrated system could provide a better understanding of the charge transfer between the anion and the water molecules, which could further aid to comprehend the anion solvation. The sum of the total NPA charges in the anion with respect to the number of water molecules in the most stable configurations are given in Table S9 and are also plotted in Fig. 7. The foregoing discussions are based on the numerical values of the NPA charges. For the OH^- anion, the sum of the total charges varies in the range from $-0.8110e((\text{OH}^-) \text{w1-h1})$ to $-0.7386e((\text{OH}^-) \text{w8-h2})$. Large charge transfer is visible for OH^- anion with eight water molecules ($-0.7386e$), which subsequently indicates better solvation. The reason for the large charge transfer and solvation in $(\text{OH}^-) \text{w8-h2}$ is likely due to the strong hydrogen bonding between anion and water molecules and the shorter bond length ($\sim 1.49 \text{ \AA}$). Likewise, among the other numerals of the water

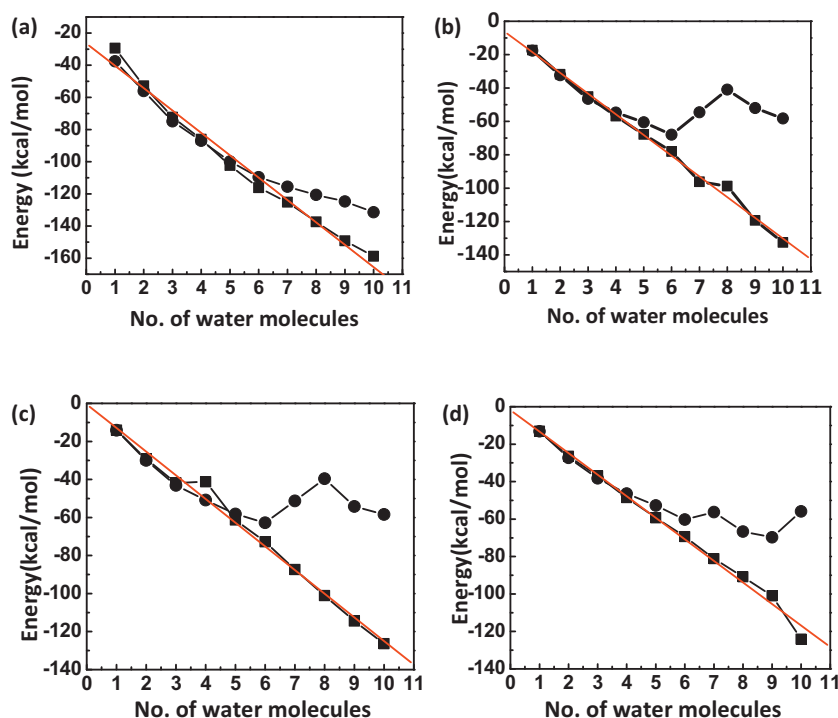


Fig. 6. (a) Variation of calculated weighted average (i) solvent stabilization energy (squares) and (ii) Interaction energy (circles) in kcal/mol with the number of water molecules (n) in $\text{OH}^- \cdot (\text{H}_2\text{O})_n$. (b) Variation of calculated weighted average (i) solvent stabilization energy (squares) and (ii) interaction energy (circles) in kcal/mol with the number of water molecules (n) in $\text{NO}_2^- \cdot (\text{H}_2\text{O})_n$. (c) Variation of calculated weighted average (i) solvent stabilization energy (squares) and (ii) interaction energy (circles) in kcal/mol with the number of water molecules (n) in $\text{NO}_3^- \cdot (\text{H}_2\text{O})_n$. (d) Variation of calculated weighted average (i) solvent stabilization energy (squares) and (ii) interaction energy (circles) in kcal/mol with the number of water molecules in $\text{CO}_3^- \cdot (\text{H}_2\text{O})_n$. Solid lines connecting the computed values are a guide to the eye. Red line is the fitted line.

molecule, 10 and 5 water molecules also provide effective solvation for the OH^- anionic structures. Further, the solvation of the anion is also evidenced through the decrease in the charge of the surrounding water molecules (shown in Table S9). In the case of NO_2^- anion, we notice a maximum charge transfer for the structure (NO_2^-) w9-h2 (−0.8411e), while similar to the OH^- anion, the minimum charge transfer is for the one water complex, namely (NO_2^-) w1-h1 (−0.9399e). However, on comparing the OH^- anion, the solvation of NO_2^- anion is slow, because of the small charge transfer between the anion and the water molecules due to the weak hydrogen bonding. For the NO_3^- anion the minimum charge transfer complex is same as that of the OH^- and NO_2^- anion, (NO_3^-) w1-h1 (−0.9681e), but the maximum charge transfer is observed

for the seven water structure (NO_3^-) w7-h1 (−0.8984e). From the NPA charge values, for both the NO_2^- and NO_3^- anions, the solvation process looks similar even though the magnitude of the total charge in NO_3^- anion is marginally higher than NO_2^- anion. This trend may be due to the similar magnitude of hydrogen bond lengths in the NO_2^- and NO_3^- anions. Finally, for the CO_3^- anion the solvation process appears to be the slowest of all the anions, because, the total charge value range between −0.9240e (in (CO_3^-) w4-h2) and −0.9766e (in (CO_3^-) w1-h2), which indicates minimal charge transfer. Moreover, this is expected as CO_3^- anion complexes possess weak hydrogen bonds. In general, on increasing the water molecules from one to ten, the solvation of the OH^- anion is rapid and requires less number of water molecules when compared with the NO_2^- , NO_3^- , and CO_3^- anions. Hence, all the above results conclude that strong hydrogen bonds augment the rapid solvation through effective charge transfer.

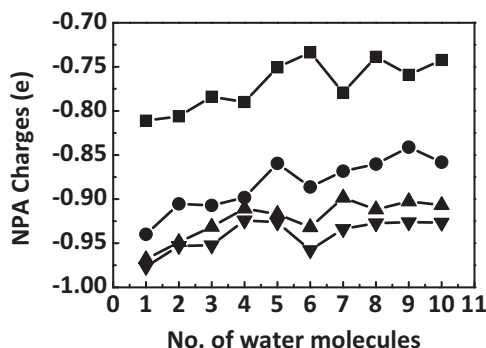


Fig. 7. Variation of NPA charges of the anions OH^- (squares), NO_2^- (circles), NO_3^- (triangles) and CO_3^- (inverted triangles) in the discrete sized hydrated clusters with the number of water molecules in the most stable anion water complexes. Solid lines connecting the computed values are a guide to the eye.

3.8. Energy decomposition analysis (EDA)

A number of EDA methods have been proposed to describe the intra or intermolecular interactions through the partition of the interaction energy. Among them, the energy decomposition scheme proposed by Su and Li [49] is known as LMO-EDA (localized molecular orbital energy decomposition analysis), which calculates the electrostatic, exchange and repulsion terms separately. This method can be successfully applied to both open-shell and closed-shell systems and insensitive to the quality of the basis sets employed [50,51]. The contribution of various energy components to the interaction energy can be expressed as:

$$\Delta E^{\text{INT}} = \Delta E^{\text{ES}} + \Delta E^{\text{EX}} + \Delta E^{\text{REP}} + \Delta E^{\text{POL}} + \Delta E^{\text{DISP}}$$

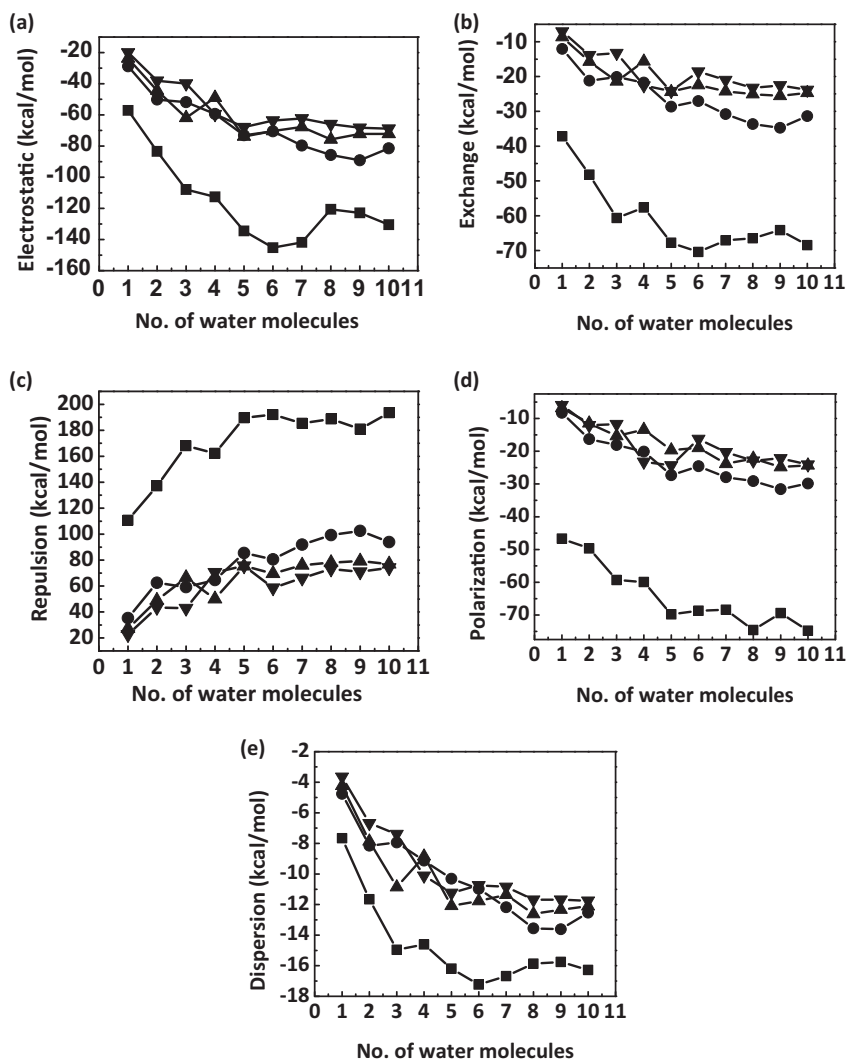


Fig. 8. (a) Plot showing the variation of electrostatic interaction (in kcal/mol) with respect to number of water molecules for most stable anionic water complexes of OH^- (squares), NO_2^- (circles), NO_3^- (triangles) and CO_3^{2-} (inverted triangles). (b) Plot showing the variation of exchange interaction (in kcal/mol) with respect to number of water molecules for most stable anionic water clusters of OH^- (squares), NO_2^- (circles), NO_3^- (triangles) and CO_3^{2-} (inverted triangles). (c) Plot showing the variation of repulsion interaction (in kcal/mol) with respect to number of water molecules for most stable anionic water clusters of OH^- (squares), NO_2^- (circles), NO_3^- (triangles) and CO_3^{2-} (inverted triangles). (d) Plot showing the variation of polarization interaction (in kcal/mol) with respect to number of water molecules for most stable anionic water clusters of OH^- (squares), NO_2^- (circles), NO_3^- (triangles) and CO_3^{2-} (inverted triangles). (e) Plot showing the variation of dispersion interaction (in kcal/mol) with respect to number of water molecules for most stable anionic water complexes of OH^- (squares), NO_2^- (circles), NO_3^- (triangles) and CO_3^{2-} (inverted triangles). Solid lines connecting the computed values are a guide to the eye.

where, ΔE^{ES} describes the electrostatic energy between the static charge densities of each monomer, ΔE^{EX} exchange energy which arises due to the antisymmetric nature of a wave function that allows electrons to exchange between the monomers, ΔE^{REP} repulsion energy, ΔE^{POL} polarization energy, also known as orbital relaxation energy, which is a major indicator of covalent nature of a bonding interaction, ΔE^{DISP} dispersion energy is an attractive term, which arises due to electron correlation [52]. In this work, the counterpoise corrected intermolecular interaction between atmospheric anions (OH^- , NO_2^- , NO_3^- and CO_3^{2-}) and water molecules are studied using EDA calculations performed at B3LYP level combined with the basis set of 6-311++G(d,p) in GAMESS software.

The LMO-EDA results for the most stable configurations of $\text{OH}^- \cdot (\text{H}_2\text{O})_n$, $\text{NO}_2^- \cdot (\text{H}_2\text{O})_n$, $\text{NO}_3^- \cdot (\text{H}_2\text{O})_n$ and $\text{CO}_3^{2-} \cdot (\text{H}_2\text{O})_n$ are tabulated in Tables S10, S11, S12 and S13 of SI, respectively. The graphical representation in Fig. 8a–e, shows the variation of the electrostatic, exchange, repulsion, polarization and dispersion components of interaction energy with respect to the number of

water molecules in $\text{OH}^- \cdot (\text{H}_2\text{O})_n$, $\text{NO}_2^- \cdot (\text{H}_2\text{O})_n$, $\text{NO}_3^- \cdot (\text{H}_2\text{O})_n$ and $\text{CO}_3^{2-} \cdot (\text{H}_2\text{O})_n$ anionic water clusters. The foregoing discussion in this section is based on the absolute energy values, although the numerical values are given in Tables S10–S13. On considering the general trend, we observe that all the attractive components of interaction energy (electrostatic, exchange, polarization and dispersion interaction), gradually increase with the increase in the number of water molecules. This increase in the attractive components of interaction energy is due to the coordination of anion with multiple numbers of water molecules, which subsequently increases the number of hydrogen bonds formed between the anion and the water molecule, resulting in the higher contribution from the attractive terms. However, this trend ceases beyond six water molecules because further increase in the cluster size results in the dominance of water–water interactions in the cluster rather than the anionic–water interactions due to smaller size of the anion. Likewise, the repulsive interaction term also increases gradually with the increase in the number of water molecules, because of

the repulsion exerted between the water molecules due to their orientations. The Basis Set Superposition Error (BSSE) corrected interaction energy values calculated through LMO-EDA method remains the same as that of counterpoise method. This validates the accuracy of the LMO-EDA scheme for interaction energy decomposition.

From Fig. 8a–e, for the OH^- anion, the curves of electrostatic, exchange, polarization and dispersion interactions are distinct from the other anions, as we observe higher magnitude for all the interaction energy components. The reason could be the strong charge transfer between the OH^- anion and the water molecule due to the donor-acceptor pair character of OH^- anion and its linear structure, which could have enhanced the interaction energy components. Subsequently, the above results accord strong binding between OH^- anion and the water molecules. However, in the case of NO_2^- , NO_3^- and CO_3^- anions, all of them show a synonymous trend for all the attractive and repulsive terms. This is due to the similarity in the interaction of NO_3^- , NO_2^- and CO_3^- anion with the water cluster. Among these three anions, NO_2^- seems to interact marginally strong with the water cluster.

On analysing the individual energy components of all the anion water complexes from Tables S10–S13, we notice that the contribution of electrostatic energy term is higher in all the clusters irrespective of the size and the anion. The electrostatic energy values vary in the range from a maximum of 141.80 kcal/mol [in $\text{OH}^-(\text{H}_2\text{O})_7$] to a minimum of 19.93 kcal/mol [in $\text{CO}_3^-(\text{H}_2\text{O})_1$]. This proves that the hydrogen bonded interactions are electrostatic in nature in all the clusters. The second dominant interactive component is the exchange interaction, found to be high in all the anions (37.19 kcal/mol to 7.05 kcal/mol). However, an interesting observation is visible in the OH^- anion, that is the exchange energy value is higher compared to all the other anions, but contrarily within the OH^- anion clusters, the polarization term is found to be higher than the exchange term. This accounts to the large charge transfer between the monomers, probably from the OH^- anion to the water molecules. Overall, except for OH^- anion the polarization energy term ranks as the third large contributor for the interaction energy in all the other anions. The dispersion interaction term provides the least contribution to the interaction energy overall, but similar to all the other interaction energy terms, has a large presence in the OH^- anion.

On comparing the interaction energy values for the structures such as OH^- w6-h2, OH^- w7-h1, NO_2^- w8-h3, NO_2^- w9-h2, NO_3^- w3-h1, NO_3^- w6-h1 and CO_3^- w6-h1, which have maximum hydrogen bonds in the first solvation shell (given in Table S10, S11, S12, S13) we observe that OH^- anion with four hydrogen bond is more attractive towards the water molecules compared to other anions. Further, among all the anions the magnitude of the interaction energy decreases with the increase in hydrogen bonds in the first solvation shell ($\text{OH}^- > \text{NO}_2^- > \text{NO}_3^- > \text{CO}_3^-$). Thus, the interaction energy profile depends upon the strength of the hydrogen bond rather than its quantity.

3.9. AIM analysis

An atom in molecule analysis (AIM) is a pioneer tool widely used for hydrogen bond characterization. In this work, we find all complexes possess O–H...O hydrogen bond and NO_2^- anionic systems have O–H...N bond in addition to O–H...O bond, hence it would be rational to analyze its topological character at the bond critical points (BCP). A Bond Critical Point (Point corresponding to $\nabla\rho=0$) is found between each pair of nuclei, which are considered to be linked by a chemical bond with two negative curvatures (λ_1 and λ_2) and one positive curvature (λ_3) denoted as the (3,–1) critical point. The bond ellipticity defined in terms of the two negative curvatures as $\epsilon=(\lambda_1/\lambda_2-1)$ reflects the deviation of the charge distribution of

a bond path from axial symmetry, thus providing a sensitive measure of the susceptibility of a system to undergo a structural change. The Laplacian of the electronic density ($\nabla^2\rho$) indicates whether the electron density is locally concentrated ($\nabla^2\rho<0$) or depleted ($\nabla^2\rho>0$) [53,54]. Popelier has proposed a set of AIM criteria that must be fulfilled for an intermolecular link to be characterized as a true hydrogen bond. Generally, the values of the electronic density and its Laplacian $\nabla^2\rho$ at the bond critical point are the two criteria applied for the existence of the Hydrogen bond. Information about the stability of hydrogen bonds can be retrieved from the bond ellipticity at the BCP. The parameters used for the O–H...O hydrogen bond characterization are the electron density (ρ in a.u.), Laplacian of the electron density $\nabla^2\rho$ (a.u.), and ellipticity (ϵ) at bond critical point (BCP). High electron density suggests strong hydrogen bonds, the Laplacian of the electron density indicates the ionic or covalent nature of the bond, while ellipticity measure distortion [55–57].

The AIM parameters for the O–H...O bond formed between anion and water molecules of the most stable configurations in $\text{OH}^-(\text{H}_2\text{O})_n$, $\text{NO}_2^-(\text{H}_2\text{O})_n$, $\text{NO}_3^-(\text{H}_2\text{O})_n$ and $\text{CO}_3^-(\text{H}_2\text{O})_n$ are tabulated in Tables S14, S15, S16 and S17 of SI, respectively. The results from the table suggest that the topological parameters fulfil the criteria as proposed by Popelier. In general, the electron density values of strong hydrogen bonds are high due to strong overlap of orbitals. Even though the bond length of DHB is greater than 2 Å, there is no significant difference in their electron density and the Laplacian of electron density values.

The positive values of the Laplacian of the electron density from Tables S14, S15, S16 and S17 are indicative of depletion of electronic charge along a bond path, which is a characteristic of closed shell interactions such as hydrogen bonds. The value of $\nabla^2\rho$ for the bare anion shows that the bonds in the anion are ionic in nature. On increasing the number of water molecules, the ionic nature of the anion is preserved, as $\nabla^2\rho<0$. The higher ellipticity values in all the anions indicate the higher possibility of structural changes under external perturbations. The correlation between the electron density at BCP and the hydrogen bond length are inverse with the correlation coefficients as 0.9723, 0.9578, 0.9201 and 0.9581 for $\text{OH}^-(\text{H}_2\text{O})_n$, $\text{NO}_2^-(\text{H}_2\text{O})_n$, $\text{NO}_3^-(\text{H}_2\text{O})_n$ and $\text{CO}_3^-(\text{H}_2\text{O})_n$ complexes respectively and are shown in Figs. S1, S3, S5, and S7. The correlation between the bond length and electron density is inverse, that is, an increase in bond length corresponds to a decrease in the electron density values, which is expected, since increase in distance results in reduced orbital overlap and hence, low electron density along the bond. Similarly, the correlation between the Laplacian of the electron density and the hydrogen bond length is inverse with the correlation coefficients as 0.9009 (excluding a point corresponding to OH^- with one water molecule), 0.9892, 0.9794 and 0.9803 for $\text{OH}^-(\text{H}_2\text{O})_n$, $\text{NO}_2^-(\text{H}_2\text{O})_n$, $\text{NO}_3^-(\text{H}_2\text{O})_n$ and $\text{CO}_3^-(\text{H}_2\text{O})_n$ respectively are shown in Figs. S2, S4, S6, and S8. The inverse correlation of Laplacian is analogous to electron density and hydrogen bond length.

3.10. NBO analysis

NBO analysis is a reliable tool to obtain information [58] about the hydrogen bonds in the form of the change in charge densities of the bonding and antibonding orbitals of proton donor and acceptor respectively. The parameters of NBO such as occupation number of lone pair and anti-bonding orbitals in proton acceptor and donor, respectively in the O–H...O bond formed between the anion and the water molecules of the most stable configurations along with the corresponding stabilization energies are tabulated in Tables S18, S19, S20 and S21 of SI. For each donor NBO (i) and acceptor

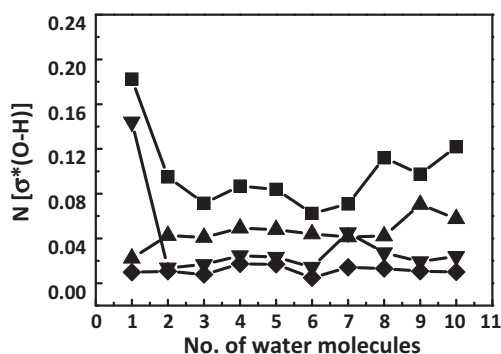


Fig. 9. Plot showing the number of water molecules accompanying the corresponding anion with respect to the Occupation number of anti-bonding orbitals of proton donor $\sigma^*[\text{O}-\text{H}]$ for the most stable anionic water clusters of OH^- (squares), NO_2^- (triangles), NO_3^- (inverted triangles) and CO_3^- (diamonds). Solid lines connecting the computed values are a guide to the eye.

NBO (j), the stabilization energy $E^{(2)}$ associated with delocalization $i \rightarrow j$ is estimated as:

$$E^{(2)} = \Delta E_{ij} = q_i \frac{F(i,j)^2}{\varepsilon_j - \varepsilon_i}$$

where q_i is the donor orbital occupancy, $\varepsilon_i, \varepsilon_j$ are diagonal elements (orbital energies) and $F(i,j)$ is the off-diagonal NBO Fock matrix element.

A graph plotted between the anti-bonding orbital occupation number of $\text{O}-\text{H} \cdots \text{O}$ for all anionic water clusters ($\text{O}-\text{H} \cdots \text{O}$ bond with higher stabilization energy is alone selected) and the number of water molecules, is shown in Fig. 9. Among the anion water complexes, OH^- anion is peculiar because it acts as donor-acceptor pair, while in all other complexes, anions are proton acceptors and water molecules act as proton donor. The charge transfer occurs from the lone pair of anions to the antibonding orbital of water molecules. Moreover, in all complexes all the hydrogen bonds formed are of $\text{O}-\text{H} \cdots \text{O}$ type. Large charge transfer from the anion to the water molecules increases the occupation number of the $\sigma^*[\text{O}-\text{H}]$ orbital of the water molecule. Subsequently, $\text{O}-\text{H}$ bond in water elongates, which in turn aids in the strong interaction between H (in water) and O atoms (in anion), resulting in shorter hydrogen bond lengths with maximum amount of stabilization energy. In addition, the maximum value of stabilization energy indicates the strength of interaction between the monomers.

The occupancy value of the oxygen lone pair in monomer anion is 1.9991e (in OH^-), 1.9923e (in NO_2^-), 1.9822e (in NO_3^-) and 0.9921e (in CO_3^-). When the anions are made to hydrated, this lone pair is transferred to water molecules that coordinate with it. The change observed in the occupancy values of lone pair of oxygen atom after hydration is in the range 1.9975e to 1.9373e (in OH^-), 1.9873e to 1.9205e (in NO_2^-), 1.9809e to 1.9716e (in NO_3^-), 0.9919e to 0.9780e (in CO_3^-). The amount of lone pair transfer can be measured from an increase in the occupancy value of $\sigma^*[\text{O}-\text{H}]$ orbital of water molecules. Here, we see that for OH^- the increase in antibonding orbital occupancy value is maximum among all anions, in the range from 0.1825e to 0.0336e. Because of this, we find a strong interaction between OH^- and water molecule as reported in the earlier paragraph. In NO_3^- the charge transfer from the oxygen atom (NO_3^-) to water molecules are in the range from 0.1441e to 0.0035e, which is second to that of OH^- anion. However, NO_2^- and CO_3^- have minimum charge transfer in the range from 0.0703e to 0.0093e and from 0.0173e to 0.0012e, respectively. The graphical representation in Fig. 9, reflects that the occupancy of $\sigma^*[\text{O}-\text{H}]$ in water molecules bonded with OH^- anion decreases initially but for water molecules beyond $n = 7$ the value increases. However, in

other anions the occupancy values remain constant. In addition, it is worth to note that there is a correlation between hydrogen bond length and the stabilization energy, which reveals that the shorter the bond length, stronger the hydrogen bond, which in turn has higher stabilization energy.

4. Conclusion

The hydrated structure of OH^- , NO_2^- , NO_3^- and CO_3^- are studied using the density functional theory calculations. Structural parameters, solvation energy, interaction energy, EDA, NPA, AIM and NBO are analyzed. Several closely lying minimum energy structures are predicted in $\text{X}^-(\text{H}_2\text{O})_n$ ($\text{X} = \text{OH}, \text{NO}_2, \text{NO}_3$ and CO_3), where $n = 1-10$. Hydrogen bonding occurs in three different ways as SHB, DHB and WHB. All the complexes are formed through $\text{O}-\text{H} \cdots \text{O}$ type hydrogen bond, in which anion acts as proton acceptors, while water molecule acts as a proton donor. A linear correlation is obtained for weighted average solvent stabilization energy with the size (n) of the hydrated cluster. From the results of weighted average interaction energy values, it is observed that the OH^- anion binds strongly with water molecules and needs a lesser number of water molecules to solvate than the other anions considered. Energy decomposition analysis performed shows that the hydrogen bonding in the anionic water clusters had a major share of electrostatic and polarization contributions, in general the hydrogen bond is of electrostatic in nature. NPA charges indicate a general decrease of the total charge in anion due to hydration. From AIM analysis, the excellent inverse correlation is found between the electron density, Laplacian of the electron density and the hydrogen bond length. Natural Bond Orbital analysis reveals large charge transfer between OH^- anion and water molecules.

Acknowledgement

One of the authors M. Lalitha thanks Bharathiar University, for providing University Research Fellowship (URF). The authors are grateful to CMSD, University of Hyderabad, India, for providing the High Performance Computing Facility (HPCF).

Appendix A. Supplementary data

Supplementary data associated with this article can be found, in the online version, at <http://dx.doi.org/10.1016/j.jmngm.2014.10.012>.

References

- [1] A.W. Castleman Jr., R.G. Keese, Clusters: properties and formation, *Annu. Rev. Phys. Chem.* 37 (1986) 525–550.
- [2] D.R. Zook, E.P. Grimsrud, Measurement of ion clustering equilibria of proton hydrates by atmospheric pressure ionization mass spectrometry, *J. Phys. Chem.* 92 (1988) 6374–6379.
- [3] S.T. Graul, M.D. Brickhouse, R.R. Squires, Deuterium isotope fractionation within protonated water clusters in the gas phase, *J. Am. Chem. Soc.* 112 (1990) 631–639.
- [4] L.G. Bjorn, F. Arnold, Mass spectrometric detection of precondensation. Nuclei at the arctic summer mesopause, *Geophys. Res. Lett.* 8 (1981) 1167–1170.
- [5] E. Arijis, D. Nevejans, J. Ingels, Stratospheric positive ion composition measurements and acetonitrile detection: a consistent picture? *Int. J. Mass Spectrom. Ion Process.* 81 (1987) 15–31.
- [6] T. Seta, M. Yamamoto, M. Nishioka, M. Sadakata, Structures of hydrated oxygen anion clusters: DFT calculations for $\text{O}^-(\text{H}_2\text{O})_n$, $\text{O}_2^-(\text{H}_2\text{O})_n$, and $\text{O}_3^-(\text{H}_2\text{O})_n$ ($n = 0-4$), *J. Phys. Chem. A* 107 (2003) 962–967.
- [7] K. Liu, J.D. Cruzan, R.J. Saykally, Water clusters, *Science* 271 (1996) 929–933.
- [8] R. Ludwig, Water from clusters to the bulk, *Angew. Chem. Int. Ed.* 40 (2001) 1808–1827.
- [9] A. Tongraar, P. Tangkawanwanit, B.M. Rode, A combined QM/MM molecular dynamics simulation study of nitrate anion (NO_3^-) in aqueous solution, *J. Phys. Chem. A* 110 (2006) 12918–12926.

- [10] X. Yang, A.W. Castleman Jr., Chemistry of large hydrated anion clusters $X^-(H_2O)_n$, $n = 0-59$ and $X = OH, O, O_2$, and O_3 . 3. Reaction of SO_2 , *J. Phys. Chem.* 95 (1991) 6182–6186.
- [11] S.A. Lyapustina, S. Xu, J.M. Nilles, K.H. Bowen Jr., Solvent-induced stabilization of the naphthalene anion by water molecules: a negative cluster ion photoelectron spectroscopic study, *J. Chem. Phys.* 112 (2000) 6643–6648.
- [12] R.P. Wayne, *Chemistry of Atmospheres*, 3rd ed., Oxford University Press, Oxford, UK, 2002.
- [13] E.E. Ferguson, F. Arnold, Ion chemistry of the stratosphere, *Acc. Chem. Res.* 14 (1981) 327–334.
- [14] A.K. Pathak, D.K. Maity, Distinctive IR signature of CO_3^{+} and CO_3^{2-} hydrated clusters: a theoretical study, *J. Phys. Chem. A* 113 (2009) 13443–13447.
- [15] A.K. Pathak, Theoretical study on microhydration of NO_3^- ion: structure and polarizability, *Chem. Phys.* 384 (2011) 52–56.
- [16] X. Yang, A.W. Castleman Jr., Production and magic numbers of large hydrated anion clusters $X^-(H_2O)_{n=0-59}$ ($X = OH, O, O_2$, and O_3) under thermal conditions, *J. Phys. Chem.* 94 (1990) 8500–8502.
- [17] D.J. Anick, Comparison of hydrated hydroperoxide anion $(HOO^-(H_2O)_n)$ clusters with alkaline hydrogen peroxide $(HOOH)(OH^-(H_2O)_{n-1})$ clusters, $n = 1-8$, 20: an ab initio study, *J. Phys. Chem. A* 115 (2011) 6327–6338.
- [18] Z. Ma, D. Anick, M.E. Tuckerman, Ab initio molecular dynamics study of the aqueous HOO^- ion, *J. Phys. Chem. B* 118 (2014) 7937–7945.
- [19] E.F. Aziz, N. Ottosson, M. Faubel, I.V. Hertel, B. Winter, Interaction between liquid water and hydroxide revealed by core-hole de-excitation, *Nat. Lett.* 455 (2008) 89–91.
- [20] Z. Ma, M.E. Tuckerman, On the connection between proton transport, structural diffusion and reorientation of the hydrated hydroxide ion as a function of temperature, *Chem. Phys. Lett.* 511 (2011) 177–182.
- [21] C.J. Mundy, I-F.W. Kuo, M.E. Tuckerman, H.-S. Lee, D.J. Tobias, Hydroxide anion at the air–water interface, *Chem. Phys. Lett.* 481 (2009) 2–8.
- [22] A. Hassanali, M.K. Prakash, H. Eshet, M. Parrinello, On the recombination of hydronium and hydroxide ions in water, *Proc. Natl. Acad. Sci. U. S. A.* 108 (51) (2011) 20410–20415.
- [23] W. Koch, M.C. Holthausen, *A Chemist's Guide to Density Functional Theory*, Wiley-VCH, New York, 2001.
- [24] L.A. Burns, Á.V. Mayagoitia, B.G. Sumpter, C.D. Sherrill, Density-functional approaches to noncovalent interactions: A comparison of dispersion corrections (DFT-D), exchange-hole dipole moment (XDM) theory, and specialized functionals, *J. Chem. Phys.* 134 (2011), 084107-1–084107-25.
- [25] S. Grimme, M. Steinmetz, *Phys. Chem. Chem. Phys.* 15 (2013) 16031–16042.
- [26] N.B. Librovich, V.P. Sakun, N.D. Sokolov, H^+ and OH^- ions in aqueous solutions. Vibrational spectra of hydrates, *Chem. Phys.* 39 (1979) 351–366.
- [27] B.R. Bickmore, K.L. Nagy, J.S. Young, J.W. Drexler, Nitrate-cancrinite precipitation on quartz sand in simulated hanford tank solutions, *Environ. Sci. Technol.* 35 (2001) 4481–4486.
- [28] A.K. Pathak, T. Mukherjee, D.K. Maity, Microhydration of NO_3^- : a theoretical study on structure, stability and IR spectra, *J. Phys. Chem. A* 112 (2008) 3399–3408.
- [29] K. Sekimoto, M. Takayama, Negative ion formation and evolution in atmospheric pressure corona discharges between point-to-plane electrodes with arbitrary needle angle, *Eur. Phys. J. D* 60 (2010) 589–599.
- [30] A. Luts, Evolution of negative small ions at enhanced ionization, *J. Geophys. Res.* 100 (1995) 1487–1496.
- [31] I. Rozas, On the nature of hydrogen bonds: an overview on computational studies and a word about patterns, *Phys. Chem. Chem. Phys.* 9 (2007) 2782–2790.
- [32] T. Kar, S. Scheiner, Comparison of cooperativity in $CH\cdots O$ and $OH\cdots O$ hydrogen bonds, *J. Phys. Chem. A* 108 (2004) 9161–9168.
- [33] O. Galvez, P.C. Gomez, Variation with the intermolecular distance of properties dependent on the electron density in hydrogen bond dimers, *J. Chem. Phys.* 115 (2001) 11166–11172.
- [34] D. Angela, Rabuck, E. Gustavo, Scuseria, Performance of recently developed kinetic energy density functional for the calculation of hydrogen binding strengths and hydrogen-bonded structures, *Theor. Chem. Acc.* 104 (2000) 439–444.
- [35] W.J. Hehre, L. Radom, Paul v.R. Schleyer, J.A. Pople, *Ab initio Molecular Orbital Theory* John Wiley and sons, vol. 1, 1986, pp. 227.
- [36] R.H. Page, M.F. Vernon, Y.R. Shen, Y.T. Lee, Infrared vibrational predissociation spectra of large water clusters, *Chem. Phys. Lett.* 141 (1987) 1–6.
- [37] E.D. Gledening, A.E., Reed, J.A., Carpenter, F. Weinhold, NBO Version 3.1.
- [38] M.J. Frisch, G.W. Trucks, H.B. Schlegel, G.E. Scuseria, M.A. Robb, J.R. Cheeseman, V.G. Zakrzewski, J.A. Montgomery, R.E. Stratmann, J.C. Burant, S. Dapprich, J.M. Millam, A.D. Daniels, K.N. Kudin, M.C. Strain, O. Farkas, J. Tomasi, V. Barone, M. Cossi, R. Cammi, B. Mennucci, C. Pomelli, C. Adamo, S. Clifford, J. Ochterski, G.A. Petersson, P.Y. Ayala, Q. Cui, K. Morokuma, D.K. Malick, A.D. Rabuck, K. Raghavachari, J.B. Foresman, J. Cioslowski, J.V. Ortiz, A.G. Baboul, B.B. Stefanov, G. Liu, A. Liashenko, P. Piskorz, I. Komaromi, R. Gomperts, R.L. Martin, D.J. Fox, T. Keith, M.A. Al-La-ham, C.Y. Peng, A. Nanoyakkara, C. Gonzales, M. Challacombe, P.M.W. Gill, B. Johnson, W. Chen, M.W. Wong, J.L. Andres, C. Gonzalez, M. Head-Gordon, E.S. Replogle, J.A. Pople, Gaussian 03. Revision A.11.2, Gaussian, Inc., Pittsburgh, 2005.
- [39] M.W. Schmidt, K.K. Baldrige, J.A. Boatz, S.T. Elbert, M.S. Gordon, J.H. Jensen, S. Koseki, N. Matsunaga, K.A. Nguyen, S.J. Su, T.L. Windus, M. Dupuis, J.A. Montgomery, General atomic and molecular electronic structure system, *J. Comput. Chem.* 14 (1993) 1347–1363.
- [40] M.S. Gordon, M.W. Schmidt, Advances in electronic structure theory. GAMESS a decade later, in: C.E. Dykstra, G. Frenking, K.S. Kim, G.E. Scuseria (Eds.), *Theory and Applications of Computational Chemistry*, Elsevier, Amsterdam, 2005.
- [41] S.B. Boys, F. Bernardi, The calculation of small molecular interactions by the differences of separate total energies. Some procedures with reduced errors, *Mol. Phys.* 19 (1970) 553.
- [42] P.L.A. Popelier, MORPHY, a program for an automated atoms in molecules analysis, *Comp. Phys. Comm.* 93 (1996) 212–240.
- [43] W.R. Busing, D.F. Horning, The effect of dissolved KBr, KOH Or HCl on the Raman spectrum of water, *J. Phys. Chem.* 65 (1961) 284–292.
- [44] P.A. Giguere, Hydrogen-bonds in aqueous-solutions of alkalis, *Rev. Chim. Miner.* 20 (1983) 588–594.
- [45] J.J. Novoa, F. Mota, C.P. del valle, M. Planas, Structure of the first solvation shell of the hydroxide anion. A model study using $OH^-(H_2O)_n$ ($n = 4, 5, 6, 7, 11, 17$) clusters, *J. Phys. Chem. A* 101 (1997) 7842–7853.
- [46] H.M. Lee, P. Tarkeshwar, K.S. Kim, Structures, energetics and spectra of hydrated hydroxide anion clusters, *J. Chem. Phys.* 121 (2004) 4657–4664.
- [47] M.E. Tuckerman, A. Chandra, D. Marx, Structure and dynamics of $OH^-(aq)$, *Acc. Chem. Res.* 39 (2006) 151–158.
- [48] S.S. Xantheas, Theoretical study of hydroxide ion–water clusters, *J. Am. Chem. Soc.* 117 (1995) 10373–10380.
- [49] P. Su, H. Li, Energy decomposition analysis of covalent bonds and intermolecular interactions, *J. Chem. Phys.* 131 (2009), 014102-1–014102-15.
- [50] S.K. Ghosh, P.K. Chattaraj, *Concepts and Methods in Modern Theoretical Chemistry: Electronic Structure and Reactivity*, CRC Press, Taylor & Francis, 2013, pp. 325–333.
- [51] A. Mano Priya, L. Senthilkumar, P. Kolandaivel, Hydrogen-bonded complexes of serotonin with methanol and ethanol: a DFT study, *Struct. Chem.* 25 (2014) 139–157.
- [52] N. Thellamurege, H. Hirao, Water complexes of cytochrome P450: insights from energy decomposition analysis, *Molecules* 18 (2013) 6782–6791.
- [53] U. Koch, P.L.A. Popelier, Characterization of C–H–O hydrogen bonds on the basis of the charge density, *J. Phys. Chem.* 99 (1995) 9747–9754.
- [54] P.L.A. Popelier, R.F.W. Bader, The existence of an intramolecular C–H–O hydrogen bond in creatine and carbamoyl sarcosine, *Chem. Phys. Lett.* 189 (1992) 542–548.
- [55] L. Senthilkumar, P. Umadevi, K.N. Sweetey Nithya, P. Kolandaivel, Density functional theory investigation of cocaine water complexes, *J. Mol. Model.* 19 (2013) 3411–3425.
- [56] L. Senthilkumar, T.K. Ghanty, S.K. Ghosh, P. Kolandaivel, Hydrogen bonding in substituted formic acid dimers, *J. Phys. Chem. A* 110 (2006) 12623–12628.
- [57] L. Senthilkumar, T.K. Ghanty, S.K. Ghosh, Electron density and energy decomposition analysis in hydrogen-bonded complexes of azabenzene with water, acetamide, and thioacetamide, *J. Phys. Chem. A* 109 (2005) 7575–7582.
- [58] V. Umadevi, L. Senthilkumar, P. Kolandaivel, Theoretical investigations on the hydrogen bonding of nitrile isomers with H_2O , HF, NH_3 and H_2S , *Mol. Simul.* 39 (2013) 908–921.